Empirical H/V spectral ratios estimated in two deep sedimentary basins using microseisms recorded by short-period seismometers

D. Bindi [1], S. Marzorati [1], S. Parolai [2], A. Strollo [2,3], and K-H. Jäkel[2,4]

(1) Istituto Nazionale di Geofisica e Vulcanologia, via Bassini 15, 20133 Milano, Italy,

(2) Helmholtz Centre Potsdam, GFZ German Research Centre for Geosciences , Telegrafenberg, 14473, Potsdam, Germany

(3) University of Potsdam, Karl-Liebknecht-Str. 24, 14476 Potsdam-Golm , Germany

(4) GIPP Geophysical Instrumental Pool Potsdam, Telegrafenberg, 14473, Potsdam, Germany

Corresponding Author:

Dino Bindi

Istituto Nazionale di Geofisica e Vulcanologia,

via Bassini 15, 20133 Milano, Italy

Tel: +39 02 23699270 Fax +39 02 23699458

e-mail: bindi@mi.ingv.it

Key words: Microseism; Site effects; Fourier Analysis; Short-period sensor; Europe

Short Title: H/V from microseism short-period data

Summary

In this work, we analyze continuous measurements of microseisms to assess the reliability of the fundamental resonance frequency estimated by means of the horizontal-to-vertical (H/V) spectral ratio within the 0.1-1 Hz frequency range, using short-period sensors (natural period of 1 sec). We apply the H/V technique to recordings of stations installed in two alluvial basins with different sedimentary cover thicknesses, the Lower Rhine Embayment (Germany) and the Gubbio Plain (Central Italy). The spectral ratios are estimated over the time-frequency domain and we discuss the reliability of the results considering both the variability of the microseism activity and the amplitude of the instrumental noise. We show that microseisms measured by short period sensors allow the retrieval of fundamental resonance frequencies greater than about 0.1-0.2 Hz, with this lower frequency bound depending on the relative amplitude of the microseism signal and the self-noise of the instruments. In particular, we show an example where the considered short-period sensor is connected to instruments characterized by an instrumental noise level which allows detecting only fundamental frequencies greater than about 0.4 Hz. Since the frequency at which the peak of the H/V spectral ratio is biased depends upon the seismic signal-to-instrument noise ratio, the power spectral amplitude of instrumental self noise should be always considered when interpreting the frequency of the peak as the fundamental resonance frequency of the investigated site.

1. Introduction

Since the beginning of instrumental seismology, ambient seismic background noise has focused the attention of many studies. It has been considered not only as an unavoidable disturbance that must be reduced to improve the utility of seismic data or the performance of a seismic network, but also as a useful signal for investigating the effect of the sub-surface geology on ground motion. Since ambient noise measurements can be rapidly performed over large areas, the possibility of linking some features extracted from the background noise recordings to the seismic response of the soil made the ambient noise a suitable tool for many studies aiming at seismic hazard assessment (Delgado et al., 2000). For example, the Nakamura technique (e.g., Nakamura, 1989) is generally applied to estimate the fundamental frequency of resonance of the site, in correspondence to the frequency of the first peak observed in the spectral ratio between the horizontal and vertical components (H/V) of noise recordings acquired at a single site. The background noise measurements can be analyzed in several ways for estimating the local site effects. In general, either the fundamental frequency of resonance estimated from single station measurements can be used to map the thickness of the soft sedimentary layer (e.g. Ibs-von Seht & Wohlenberg, 1999) or the H/V spectral ratio can be used to unravel the sub-soil structure through an inversion procedure (e.g. Fäh et al., 2003). Other studies exploited the availability of simultaneous measurements of ambient noise at an array of stations to derive a vertical shear wave velocity profile by dispersion wave analysis (e.g., Scherbaum et al., 2003; Arai & Tokimatsu, 2005; Parolai et al., 2005; Picozzi et al., 2005). Regardless of the methodology applied, any bias introduced by the adopted instrumental equipments in the background noise measurements can affect the shape of the H/V ratio and therefore corrupt the information on the sub-soil structure. The possibility of obtaining reliable site effects estimation from numerical simulation will be thus limited.

The frequency range of engineering interest generally spans the range 0.1-20 Hz. While frequencies larger than 1Hz are amplified by thin soft sediment layers and correspond to the natural period of most of the buildings, frequencies below 1 Hz are amplified by sediments thicker than about 100 m and are of interest for the response of long bridges and tall buildings (more than 10 stories high, as rule of thumb). Within this frequency range, the sources generating the background seismic noise have different nature (e.g. Webb, 1998; McNamara & Buland, 2004): while for frequencies larger than about 1 Hz the noise spectrum is related to human activities, in the frequency range from 0.1 to 1 Hz it is characterized by features related to microseism activity, generated by ocean wave energy coupling into motion of the earth (e.g. Longuet-Higgins, 1950; Bromirski et al., 2005).

Since the recordings of the background noise for engineering seismology investigations generally consist of short time measurements (for some minutes to about 1 hour) repeated at several locations over a wide urban area, short-period sensors are more suitable for these field surveys since they are less demanding than broad band instruments by the point of view of installation. However, these sensors damp the signal below their natural frequency (>=1 Hz), and then the signal amplitude may become smaller than the self-noise of the acquisition system. Under these circumstances, the signal-to-noise ratio (here indicating the ratio between the seismic noise signal and the self-noise of the acquisition system) is not improved by removing the instrumental response from the data, since the application of the instrumental correction can only lead to amplification of the self-noise. Following a theoretical approach based on numerical simulations, Strollo et al. (2008) evaluated the bias introduced by the instrumental self-noise both on the seismic noise recordings and on the horizontal-to-vertical spectral ratio (H/V) results, considering frequencies less than 1Hz. Here, the suitability of short-period recordings for estimating the fundamental resonance frequency in the 0.1-1 Hz frequency range by H/V ratio is investigated analysing empirical data collected during field experiments carried out in two alluvial basins, the Lower Rhine Embayment (Germany) and the Gubbio Plain (Central Apennines, Italy). In particular data from sites with fundamental resonance frequency less than 1 Hz, as estimated by studies (e.g. Parolai et al., 2004), are considered.

First, the time variability of the power spectra computed for ambient noise, considering high and low microseismic activity periods, and taking into account the effect of self-noise of the instruments is investigated. Second, the Nakamura technique is applied to the recordings to estimate the fundamental resonance frequency of the sites and to investigate the stability of the results against time. The analysis of the results is carried out taking into account both the variability of the microseism activity, and therefore the strength of the seismic noise signal, and the limits introduced by the employed instruments as theoretically predicted by Strollo et al. (2008).

2. Data sets

2.1 Cologne data set

We use the dataset of recordings collected within the DFNK (German Research Network for Natural Disasters) project that aimed at the investigation of site effects in the Cologne area (Parolai et al. 2001; Parolai et al., 2002; Parolai et al., 2004). A temporary network of 44 stations was deployed between 23 April to 13 June 2001 and continuously recorded background seismic noise as well as regional earthquakes and teleseisms. In the present work, we analyze data from 5 stations of the network, namely stations K13, K25, K32, K33 and K38 (Figure 1). The first four stations were equipped with PDAS TELEDYNE Geotech recording stations connected to a Mark L4C-3D sensor, while a Güralp CMG-3ESPD recording station (all in one) was installed at site K38. Data were recorded with a sample rate of 100 sps at PDAS sites and 50 sps at the Güralp site. The main characteristics of the installations can be found in (Parolai et al., 2004, Table 1). We selected these five sites because of their fundamental resonance frequency which, for stations K33, K32, K13 and K25, are less than 0.2 Hz, between 0.3 and 0.4 Hz, about 0.5 Hz, and between 0.8 and 0.9 Hz, respectively. Details are given in Parolai et al., (2004, Figure 4). The sediment thickness below these stations can be estimated using the thickness versus fundamental frequency relationship derived by Parolai et al. (2002) for the study area (i.e. $z=108f^{-1.551}$). For station K33 the estimated thickness is grater than 1.3 km; for stations K32, K13 and K25 the thickness is about 550, 320, and 130 m, respectively.

2.2 Gubbio data set

We use the recordings from three (GU07, GU09, GU10) of the stations installed in the Gubbio basin (Figure 1) by the GeoForshungsZentrum (GFZ) within the framework of a project of the Italian Dipartmento di Protezione Civile (DPC) and the Istituto Nazionale di Geofisica e Vulcanologia (INGV) aimed at computing ground-motion scenarios for some strategic areas in Italy (http://esse3.mi.ingv.it). The selected stations belong to an almost linear array crossing the basin in a north-south direction along the minor axis of the basin, which has an ellipsoidal shape (Figure1). Since station GU10 was installed on outcropping bedrock along the southern basin edge, it is not affected by significant site effects and it can be used as reference station. Stations GU07 and GU09 were placed in the basin and their fundamental resonance frequencies were estimated to be between 0.3 and 0.4 Hz, and between 0.5 and 0.6 Hz, respectively (Project DPC-INGV S3, 2007). The sediment thickness estimated for stations GU07 and GU09 is 680 m and 420 m, respectively. From June to the middle of September 2005, the sites were equipped with REFTEK 72A recording stations with a Mark L4C-3D sensor, and then until December 2005, the REFTEK digitizers were substituted with Earth Data Logger PR6-24 (EDL) digitizers. Data were recorded with a sample rate of 100 sps.

3. Data processing

We first investigate the variation of the background seismic noise by computing the Probability Density Function (PDF) for a set of Power Spectral Densities (PSDs), following McNamara & Buland (2004). We processed time series T_1 s long, from which we removed the mean and the instrumental response. Each time series is divided into segments of T_2 s, overlapping by 75%, to reduce the variance in the PSD calculation (Cooley & Tukey, 1965). The length of the time windows are T_1= 900 s and T_2= 300 s for the Cologne dataset, and T_1= 600 s and T_2= 240 s for the Gubbio dataset. The total power, representing the PSD estimate, is obtained from the square of the amplitude spectrum multiplied by the standard normalization factor $2\Delta t/N$, where Δt is the sample interval and N is the number of samples (McNamara & Buland, 2004). The PSD obtained for each T_1 s time series is estimated as the average of the PSDs computed for each T_2 s segments and converted into decibels with respect to acceleration $(m/s^2)^2/Hz$. Following McNamara & Buland (2004), we compute a distribution of probability at re-sampled discrete frequencies Fc evenly spaced on a logarithmic scale. Each frequency Fc is selected as the geometric mean frequency within a one octave interval, i.e., $Fc = (F1 * F2)^{0.5}$, where the considered interval extends from frequency F1 to F2 = 2F1. The next Fc is then computed by shifting the interval by one-sixteenth of an octave. Powers are averaged over ±10% of Fc and grouped into bins 1-dB wide and the frequency distribution at each Fc results from the number of spectral estimates that fall into a bin divided the total number of spectral estimates.

We then use the computed PSDs to investigate the time dependence of the site effects estimated from the noise recordings. The fundamental resonance frequency is estimated as the frequency corresponding to the peak of the Nakamura ratio (Nakamura, 1989), computed as the square root of the spectral ratio between the horizontal and vertical (H/V) PSDs.

4. Analysis of the Cologne dataset

Broad-band station

We use the broad-band station K38, installed in the cellar of the Wissersheim church, as the reference station for analyzing the power spectra characteristics in the Cologne area. Figure 2 shows the PSDs computed for station K38, over the period from 4 May to 11 June, 2001. The PSDs (vertical component, V) for T_1 s time series selected at the beginning of each hour are shown. Following Bromirski et al (2005), Figure 2 shows the PSD normalized to the average PSD computed over the entire time period. Several characteristics of the noise spectrum that have been observed worldwide are also recognizable for K38. For frequencies larger than 2 Hz, the background noise is dominated by anthropic sources (e.g., McNamara & Buland, 2004) as shown by the daily cycle of the noise spectrum. Spectral levels during the night time are lower by about 40 dB than the day time, when human activities are more intense. A weekly cycle is also recognizable, with lower spectral values during the weekend. The PSDs in the range 0.1-1 Hz do not show such cycles since, in this frequency band, the PSDs are dominated by the microseisms. For stations installed in Germany, the dominant sources are along the British and Norwegian coasts (Friedrich et al., 1998; Essen et al, 2003). This is shown by Figure 3 (left), which compares the PSD computed when the microseism activity was intense (May 17, 2001 julian day 137, at high noon) with the PSD of a quiet day (May 25, 2001 julian day 145 at high noon). The surface pressure maps provided by the Met-Office (Figure 3) show that larger PSD are observed when a low-pressure system was present in the north Atlantic Ocean (May 17, 2001). In particular, the microseism activity increases both the horizontal (north-south component, NS) and vertical spectral values for frequencies less than 0.5 Hz. The amplitude of the double frequency peak at about 0.2-0.3 Hz is increased by about 8-10 dB and during days of strong microseism activity a primary peak at about 0.15 Hz is also recognizable in the vertical component.

The variability in the spectral levels during the analysed period can affect the H/V spectral ratio and, consequently, bias the H/V peak, leading to incorrect assessments of the local site effects. Figure 4 (top) shows the H/V computed for station K38 equipped with a broad-band sensor. Hereinafter the H/V spectral ratio is computed as the spectral ratio between the NS and V components (NS/V). Since the main conclusions with respect to the aims of the present work, that is the assessment of the influence of the instrumental choices on the reliability of the estimated site effects, are the same when considering also the east-west (EW) horizontal component, we show the results only for the NS component.

The distribution of frequencies corresponding to the maximum amplification factor in the frequency range 0.1-1 Hz has mean value of 0.18 and standard deviation 0.01. The mean value is in good agreement with the fundamental resonance frequency estimated by Parolai et al. (2001, Figure 12).

The peak of the H/V is generally well recognizable during the analyzed period. In any case, during the days of weak microseism activity (e.g. days 135 and 151) the amplitude of the peak is about half than the amplitude observed during strong microseisms (Figure 4, middle panel) and its width at half maximum height increases to about 0.024 Hz, increasing the uncertainty of the fundamental resonance frequency retrieved.

Short-period stations

Since the reduction of the amplitude of the signal level during days of low microseism activity could affect the H/V ratio (Strollo et al., 2008), the next step consists of evaluating the reliability of the H/V spectral ratio computed using recordings from short period sensors.

Figures 5 and 6 show the results obtained for the stations K33 and K25 in the Cologne area. The figures show the PSD computed over the analyzed period for the NS (top left) and vertical (middle left) components, as well as the corresponding PDFs (top and middle right panels). The bottom panels show the NS/V ratio as a function of time and frequency (left) and the mean +/- one standard deviation of the spectral ratios computed over the whole period (right). Figure 7 shows the NS/V ratios for stations K32 and K13. The frequencies corresponding to the H/V peak are 0.17, 0.49, 0.49, 0.87 Hz for stations K33, K32, K13 and K25, respectively, in good agreement with the results obtained by Parolai et al. (2004). The figures show that the NS/V spectral ratios for all stations are quite stable over time, with only the peak for station K33 being not well expressed during days of low microseismic activity (e.g. julian days 135, and between 150 to 153) while the peak of station K13 is partially affected by the strong noise present in the horizontal spectrum at frequencies lower than the fundamental one. The strong peak at 2 Hz in the NS/V ratio of station K13 is determined by a strong industrial source of noise present in the area close to the station (Parolai et al., 2004)

To assess the influence of instrumental noise on the computed ratios, the vertical PDFs are compared to the theoretical self-noise power spectral density, as computed by Strollo et al. (2008). Assuming for the sake of simplicity that the self–noise starts to affect the PSD when the difference between the 5-th percentile (pink curves in figure 5) of the PDF distribution and the self-noise PSD becomes almost constant for decreasing frequencies, the comparison shows that the seismic noise spectral levels can also be retrieved for frequencies down to approximately 0.15-0.2 Hz, for the case of a weak microseism activity,confirming that the level of signal is strong enough to permit a reliable estimate of the fundamental resonance frequency for the characteristics of the employed instrumental equipments.

5. Analysis of the Gubbio dataset

The acquisition of seismic data in Gubbio lasted from June 2005 until April 2006. In this work we analyzed data recorded at three stations (Figure 1) during two different time periods. The first period was from 12 to 16 July 2005, when microseism activity was weak, while the second period (from 29 November to 5 December 2005) was selected during winter days when microseism activity was stronger.

Figure 8 shows the PSD computed for the north-south and vertical components of recordings at stations GU10, GU09 and GU07. Differently from the analysis performed for the Cologne dataset, the PSD in Figure 8 are not normalize to the average computed over the entire period, so as to make the comparison between the spectral levels observed within and outside the basin easier. Since station GU10 is installed on the rock outcropping on the southern edge of the basin, its spectral levels are almost free from site amplification effects and the PSD in Figure 8 can be used as reference to evaluate the amplifications occurring within the basin.

In the first period (left panels), a weak microseism occurs between 192 and 194 Julian day, while strong microseism activity is recognizable in the second period. The difference between the frequency content of microseisms in the second period could be related to the location of the source area (Stephen et al., 2003; Bromirski et al., 2005). Indeed, microseisms at frequencies larger than about 0.3 Hz are generally observed for events generated in the Mediterranean sea while lower frequencies are affected by microseisms generated in the north Atlantic (Marzorati & Bindi, 2006). Figure 8 shows that strong amplifications affect both the horizontal and vertical components of stations GU09 and GU07. Note that during the first period a constant high spectral amplitude affects frequencies lower than 0.15-0.12 Hz, hinting to a signal dominated by instrumental noise.

The NS/V spectral ratios for stations GU07 and GU09 are shown in Figure 9. The fundamental resonance frequency of the soil column below these stations is about 0.30 and 0.55 Hz, respectively. The stability over time of the estimated fundamental resonance frequency is different for the two stations. While for station GU09 it is almost the same for the two periods, the results for GU07 strongly depends upon the level of microseism activity. Although the peak is clear and stable during the whole second period, within the first period it is recognizable only when the microseism activity becomes more intense (julian days from 192 to 194). In particular, the maximum of the peak of amplification obtained for GU07 during the first period occurs at a higher frequency (0.4 Hz) than that obtained during strong microseism activity (0.3 Hz). This is confirmed by Figure 10 which shows the average NS/V for stations GU07 and GU09 computed during the two analyzed periods. For station GU09, the fundamental resonance frequency estimated during the two periods is the same but the average amplitude of the NS/V peak is smaller for period 1. For station GU07, the mean peak of the NS/V ratio during the first period is clearly shifted towards higher frequencies and its amplitude is less than that obtained from the second period recordings. In figure 10, the NS/V from background noise are also compared with the average NS/V computed when considering the recording of 27 local earthquakes with magnitudes Ml between 0.8 and 4.7 (Project DPC-INGV S3, 2007). A better agreement between the peak of the H/V spectral ratio estimated from noise recordings and from the earthquake is obtained using the noise recordings collected during the second period (strong microseism activity).

The variability of the results obtained for the stations installed in the Gubbio Plain confirms that the reliability of the amplification peak in the range 0.1-1 Hz detected by NS/V spectral ratios evaluated from short period recordings depends upon the ratio between the signal at frequencies close to resonance and the self-noise of the instrument. Figure 11 shows the mean and the 5^{th} percentile of the vertical component PDF distribution for GU07 computed considering days from 192 to 194 during the first period (period 1A), when weak microseism activity was present, from 195 to 197 in the first period (period 1B), when the microseisms activity was very quite, and from 334 to 336 in the second period (period 2), when microseism activity was intense. We recall that during period 2, the station was equipped with a sensor-acquisition system couple having a self-noise level lower than that used during period 1 (Strollo et al., 2008).

During the second period, the combination of high amplitude signal and low instrumental self-noise allow for the detection of reliable amplification patterns for frequencies greater than about 0.15 Hz, while during periods 1A and 1B, the higher instrumental self-noise limits the exploitable frequency range to those larger than about 0.35 Hz. This limit on the exploitable frequency range explains the results of Figure 10 for GU07, where during the second period, the peak around 0.3 Hz could be correctly detected because of the favourable signal to noise ratio (where the signal is the ambient noise and noise is the instrumental noise), whereas during period 1 correct information about site amplification cannot be retrieved below 0.35 Hz. A similar behaviour (apparent shift of the NS/V peak towards higher frequencies with decreasing signal-to-noise ratio) was predicted by Strollo et al. (2008) by modelling the instrumental self noise of some short period sensors-digitizer pairs.

6. Conclusions

In the present work, continuous measurements of microseisms were exploited to assess the reliability of the fundamental resonance frequency detected using short-period sensors when significant local site effects are expected at frequencies less than 1 Hz. The horizontal to vertical ratio has been computed for stations installed over sediments with different thickness and the stability over time of the results has been investigated.

Following the numerical results provided by Strollo et al. (2008), reliable H/V peak can be retrieved only if the signal-to-noise spectral ratio (SNR) at frequencies corresponding to the H/V peak (resonance frequency) is greater than a given threshold (e.g. 3). In the case analyzed here, the SNR is determined by the ratio between ambient and instrumental noise spectral levels. Since the short-period sensor filters the input signal at frequencies lower than its corner frequency (1Hz for the short-period sensor consider in the present work) and the instrumental self-noise spectral level increases for decreasing frequency (e.g. Strollo et al., 2008), the SNR decreases with decreasing frequency and fundamental frequencies of resonance occurring at frequencies below a threshold cannot be retrieved. As shown by the results obtained for station GU07 in the Gubbio basin, this threshold can be lowered by diminishing as much as possible the instrumental self-noise and performing the measurements during hours of strong ambient noise. But, while the self-noise can be partially attenuated by selecting an appropriate set-up for the adopted instrumental equipment (e.g., by increasing as much as possible the gain of digitizers, as suggested by Strollo et al., 2008), the environmental condition are not under the control of the operator. This means that, for a given instrumental choice, the results could be not reproducible, since depending on the input signal, and biased estimates of the fundamental frequency of resonance are obtained. This is the result shown in this article for GU07 when comparing the H/V computed during period 1 (low microseism activity) with the transfer function obtained by analyzing the recorded earthquakes. The peak is clearly shifted towards high frequencies and strongly attenuated (Figure 10) and, without any further information, the low amplification of the peak could cast doubts about its reliability. The risk of completely missing the peak of resonance at frequency below 1 Hz is increased if short-period sensor with corner frequencies higher than 1 Hz (e.g. considering the 4.5 Hz geophones, frequently used in microzonation projects) are adopted (Strollo et al., 2008). In conclusion, for a correct interpretation of the amplification peaks at frequencies less than 1 Hz estimated using recordings from short-period sensors, an estimate of the ambient noise-to-instrumental noise ratio must always be considered.

Acknowledgements

We would like to thank the UK Met-Office (http://www.metoffice.org) for making available the surface pressure analysis charts shown in Figure 3. These charts are subject to Crown copyright 2005, published by the Met-Office. We also thank the Associate Editor T. Minshull and two anonymous reviewers for their constructive comments.

References

Bromirski, P. D., F. K. Duennebier, & Stephen, R. A., 2005. Mid-ocean microseisms, Geochem. Geophys. Geosyst., 6, Q04009, doi:10.1029/2004GC000768.

Cooley, J. W., & Tukey, J. W., 1965. An algorithm for machine calculation of complex Fourier series, Math. Comput., 19, 297–301

Delgado, J., C. Lopez Casado, J. Giner, A. Estevez, A. Cuenca, & Molina, S., 2000. Microtremors as a geophysical exploration tool: applications and limitations, Pure Appl. Geophys. 157, 1445–1462.

Essen, H.-H., Krüger, F., Dahm,T. & Grevemeyer, I., 2003. On the generation of secondary microseisms observed in northern and central Europe, J. geophys. Res., 108(B10), 2506, doi:10.1029/2002JB002338.

Fäh, D., Kind, F. & Giardini, D., 2003. Inversion of local S-wave velocity structures from average H/V ratios, and their use for the estimation of site-effects. Journal of Seismology 7, 449–467.

Friedrich, A., F. Krüger, & Klinge, K., 1998. Ocean generated microseismic noise located with the Gräfenberg array, J. Seismol., 2, 47–64.

Ibs-von Seht, M., & Wohlenberg, J., 1999. Microtremor measurements used to map thickness of soft sediments, Bull. Seism. Soc. Am. 89, 250–259.

Longuet-Higgins, M. S., 1950. A theory of the origin of microseisms, Philos. Trans. R. Soc. London, Ser. A, 243, 2–36.

Marzorati, S., & Bindi, D., 2006. Ambient noise levels in north central Italy, Geochem. Geophys. Geosyst., 7, Q09010, doi:10.1029/2006GC001256.

McNamara, D. E., & Buland, R. P., 2004. Ambient noise levels in the continental United States, Bull. Seismol. Soc. Am., 94(4), 1517–1527.

Nakamura, Y., 1989. A method for dynamic characteristics estimation of subsurface using microtremor on the ground surface, Q. Rep. Railway Tech. Res. Inst. Tokyo 30, 25–33.

Parolai, S., Bormann, P. & Milkereit, C., 2001. Assessment of the natural frequency of the sedimentary cover in the Cologne area (Germany) using noise measurements, J. Earthquake Eng., 5(4), 541-564.

Parolai, S., Bormann, P., & Milkereit, C., 2002. New relationships between Vs, thickness of the sediments and resonance frequency calculated by means of H/V ratio of seismic noise for the Cologne area (Germany), Bull. Seismol. Soc. Am. 92 (6), 2521– 2527.

Parolai, S., Richwalski, S.M., Milkereit, C. & Bormann, P., 2004. Assessment of the stability of H/V spectral ratios and comparison with earthquake data in the Cologne area (Germany). Tectonophysics, 390, 57-73.

Parolai, S., M. Picozzi, S.M. Richwalski, & Milkereit, C., 2005. Joint inversion of phase velocity dispersion and H/V ratio curves from seismic noise recordings using a genetic algorithm, considering higher modes. Geoph. Res. Lett., 32, doi: 10.1029/2004GL021115.

Picozzi, M., S. Parolai, & Richwalski, S. M., 2005. Joint inversion of H/V ratios and dispersion curves from seismic noise: estimatine the S-wave velocity of bedrock. Geoph. Res. Lett., 32, doi: 10.1029/2005GL022878.

Project DPC-INGV S3 (2007), Shaking scenarios including site effects, Deliverables D22-D23, Task 6-Gubbio test site, http://esse3.mi.ingv.it

Scherbaum, F., K.-G. Hinzen, & Ohrnberger, M., 2003. Determination of shallow shear wave velocity profiles in Cologne, Germany area using ambient vibrations, Geophys. J. Int., 152, 597-612.

Stephen, R. A., F. N. Spiess, J. A. Collins, J. A. Hildebrand, J. A. Orcutt, K. R. Peal, F. L. Vernon, & Wooding, F. B., 2003. Ocean Seismic Network Pilot Experiment, Geochem. Geophys. Geosyst., 4(10) , 1092, doi:10.1029/2002GC000485.

Strollo A, S. Parolai, K-H. Jäkel, S. Marzorati, & Bindi, D., 2008. Suitability of short-period sensors for retrieving reliable H/V peaks for frequencies less than 1 Hz, Bull. Seism. Soc. Am., 98, 671–681, doi: 10.1785/0120070055

Webb, S.C., 1998. Broadband seismology and noise under the ocean, Reviews of Geophysics, 36, 105-142

Figure captions

Figure 1. Top: The large circles indicate the stations analyzed in the present work (K38, K33, K32, K25 and K13), selected among those analyzed by Parolai et al. (2004) in the Lower Rhine Embayment (Germany). Small empty circles are short-period stations; black triangles are broad-band stations. Bottom: Simplified geological map of the Gubbio plain (Central Italy). Grey circles: seismic stations installed within the DPC-INGV project; black circles: stations considered in the present work.

Figure 2. Power Spectral Density (PSD) in acceleration for station K38 (Wisserheim church), vertical component. Day 124 is a Friday. For each frequency, the PSD minus the average PSD computed over the entire period is shown.

Figure 3. Top: PSD computed for station K38, considering the NS (broken line) and V (solid line) components. Red lines: 25 May, 2001 (julian day 145) at high noon; blue lines: May 17, 2001 (julian day 137) at high noon. Middle: Surface pressure chart of May 17, 2001 (julian day 137) indicating unstable weather conditions. Bottom: Surface pressure chart of May 25, 2001 (julian day 145) indicating stable weather conditions.

Figure 4. Top: NS over Vertical spectral ratios for station K38. Middle: amplitude of the NS/V peak, averaged over one day. Bottom: width at half maximum height of the NS/V peak, averaged over one day.

Figure 5. Station K33. Top: PSD (left) and Probability Density Function (PDF) (right) for component NS. The 5th percentile of the PDF is also shown (pink curve). Middle: PSD (left) and PDF (right) for component V. The theoretical self-noise PSD (Strollo et al., 2008) (black curve) and the 5th percentile of the PDF (pink curve) are also shown. Bottom: NS/V spectral ratios in the time-frequency domain (left) and average ± 1 standard deviation spectral ratio computed over the whole period (right).

Figure 6. The same as in Figure 5 but for station K25.

Figure 7. NS/V spectral ratios in the time-frequency domain (left) and average ± 1 standard deviation spectral ratio computed over the whole period (right) for stations K13 (top) and K32 (bottom).

Figure 8. PSDs computed for components NS and V recorded at stations GU10, GU09, GU07, from top to bottom respectively. Left: period 1 (12-16 July, 2005). Right: period 2 (29 November-5 December, 2005).

Figure 9. NS/V spectral ratios for stations GU09 (top panels) and GU07 (bottom panels) over the period 12-16 July and 29 November-5 December, 2005.

Figure 10. Average NS/V spectral ratios computed over period 1 (broken line), period 2 (solid black line) and considering 27 earthquake recordings (red line). Left: station GU07; right: station GU09.

Figure 11. Power spectral densities (PSD) for station GU07, vertical component. Broken line: 5th percentile of the Probability Density Function (PDF); solid line: mean PDF. Different colours correspond to different periods. 1st period A: first period with microseisms, julian days from 192 to 194 (i.e. 12 to 14 July 2005); 1st period B: first period without significant microseism activity, julian days from 195 to 197 (i.e. 15 to 17 July 2005); 2nd period: julian days from 334 to 336 (i.e. from 29 November to 5 December 2005), when microseism activity was stronger.

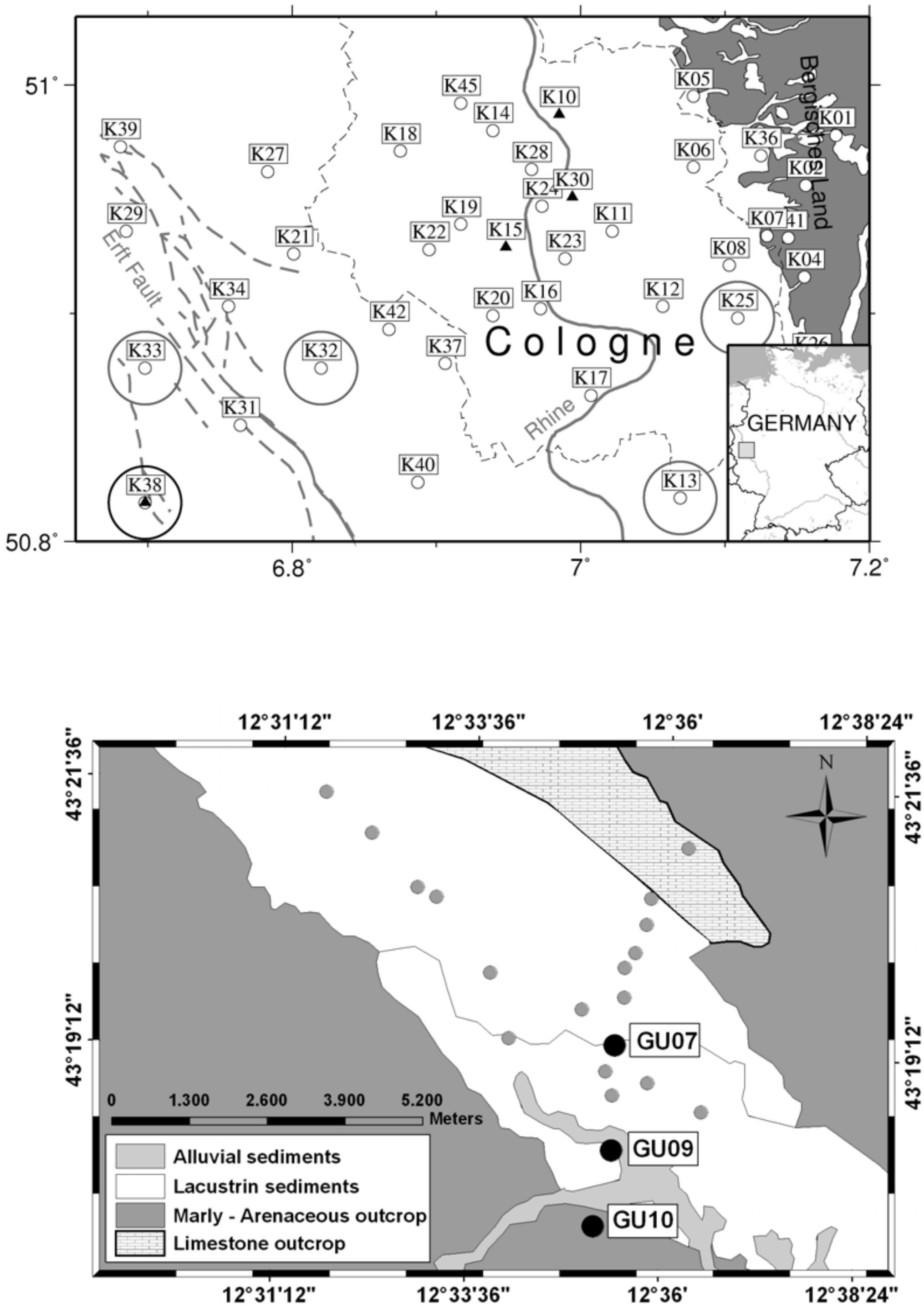
51°
50.8°
6.8°
7°
7.2°
K01
K02
K04
K05
K06
K07
K08
K10
K11
K12
K13
K14
K15
K16
K17
K18
K19
K20
K21
K22
K23
K24
K25
K27
K28
K29
K30
K31
K32
K33
K34
K36
K37
K38
K39
K40
K42
K45
Bergisches Land
Erft Fault
Cologne
Rhine
GERMANY
12°31'12"
12°33'36"
12°36'
12°38'24"
43°21'36"
43°19'12"
N
0
1.300
2.600
3.900
5.200
Meters
GU07
GU09
GU10
Alluvial sediments
Lacustrin sediments
Marly - Arenaceous outcrop
Limestone outcrop

Figure 1

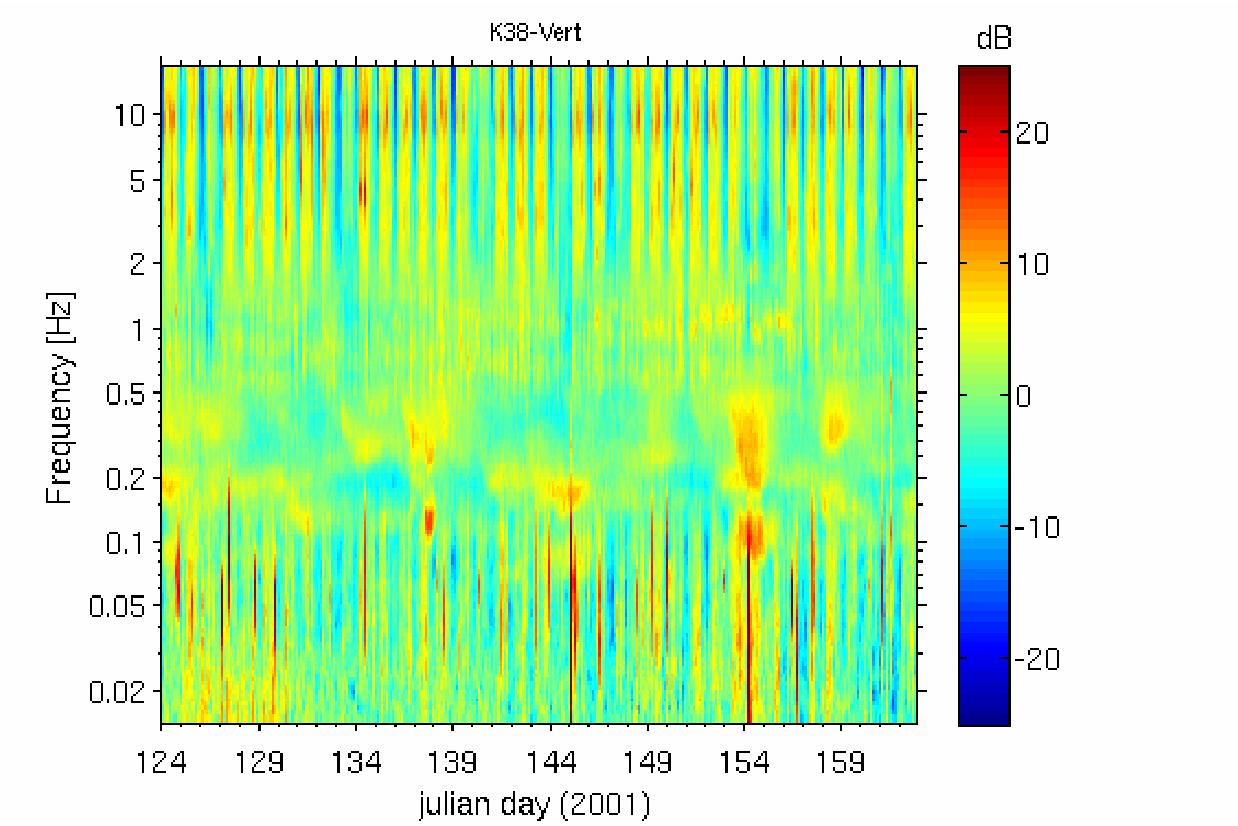
K38-Vert
dB
Frequency [Hz]
10
5
2
1
0.5
0.2
0.1
0.05
0.02
124
129
134
139
144
149
154
159
julian day (2001)
20
10
0
-10
-20

Figure 2

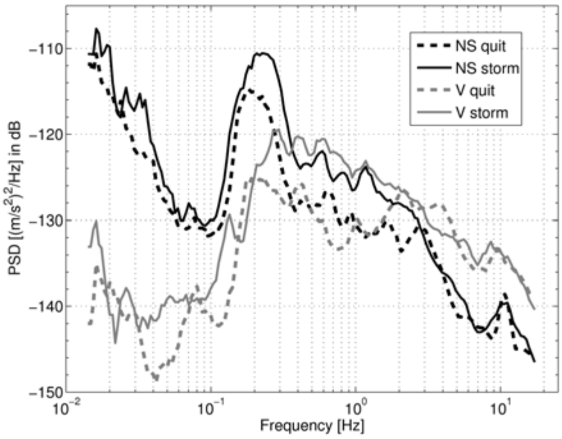
NS quit
NS storm
V quit
V storm
PSD [(m/s²)²/Hz] in dB
Frequency [Hz]
−110
−120
−130
−140
−150
10^−2
10^−1
10^0
10^1

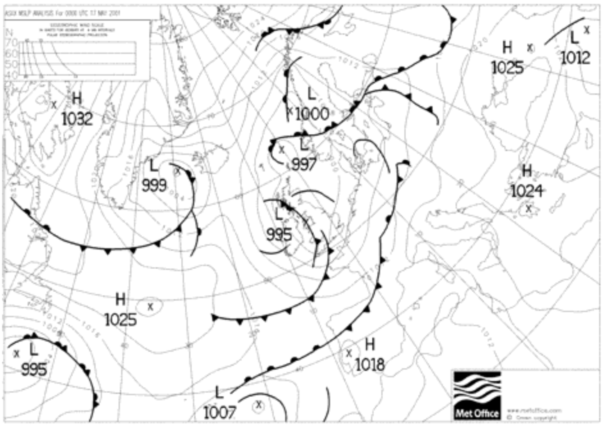
H 1025
L 1012
H 1032
L 1000
L 997
L 999
H 1024
L 995
H 1025
L 995
H 1018
L 1007
Met Office

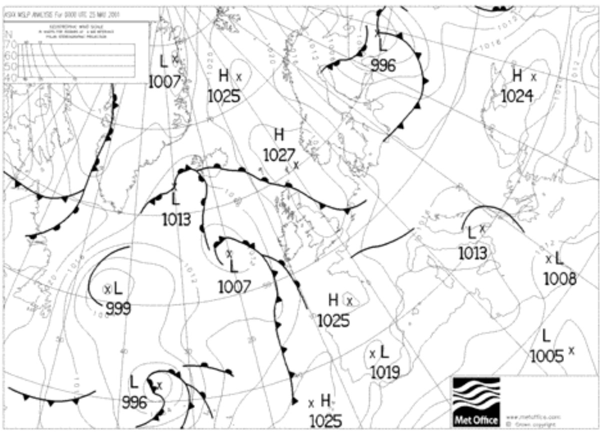
L 1007
H 1025
L 996
H 1024
H 1027
L 1013
L 1013
L 1007
L 1008
L 999
H 1025
L 1019
L 1005
L 996
H 1025
Met Office

Figure 3

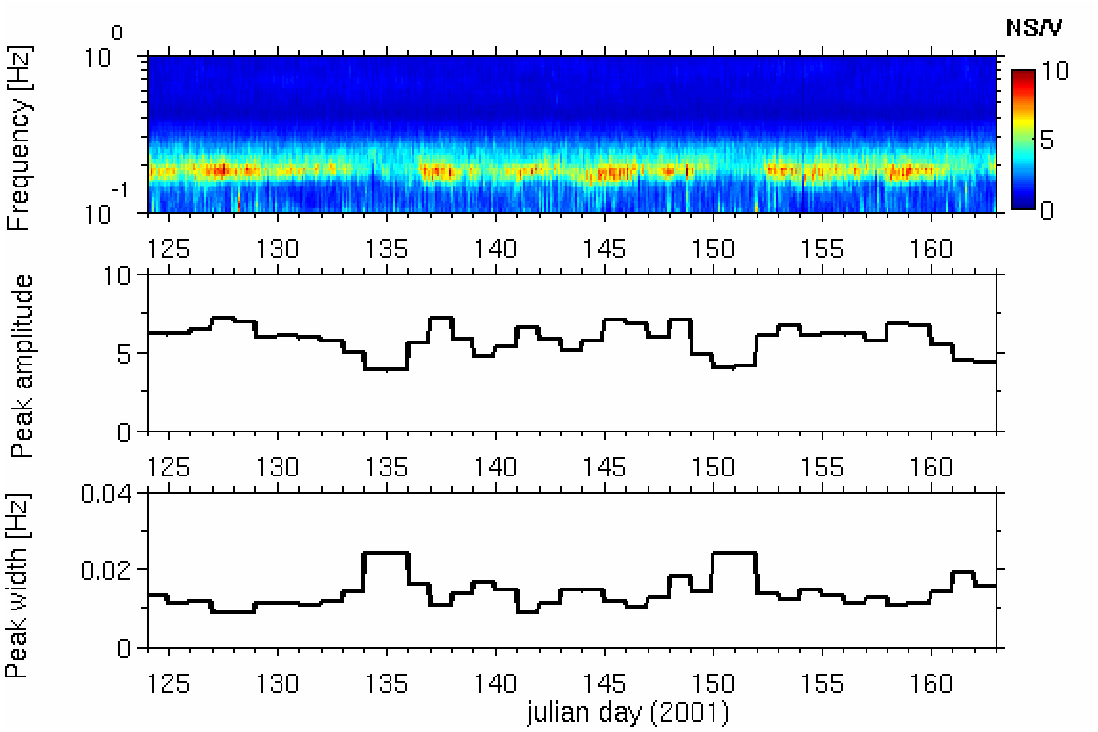

NS/V
Frequency [Hz]
10^0
10^-1
10
5
0
125
130
135
140
145
150
155
160
Peak amplitude
10
5
0
Peak width [Hz]
0.04
0.02
0
julian day (2001)

Figure 4

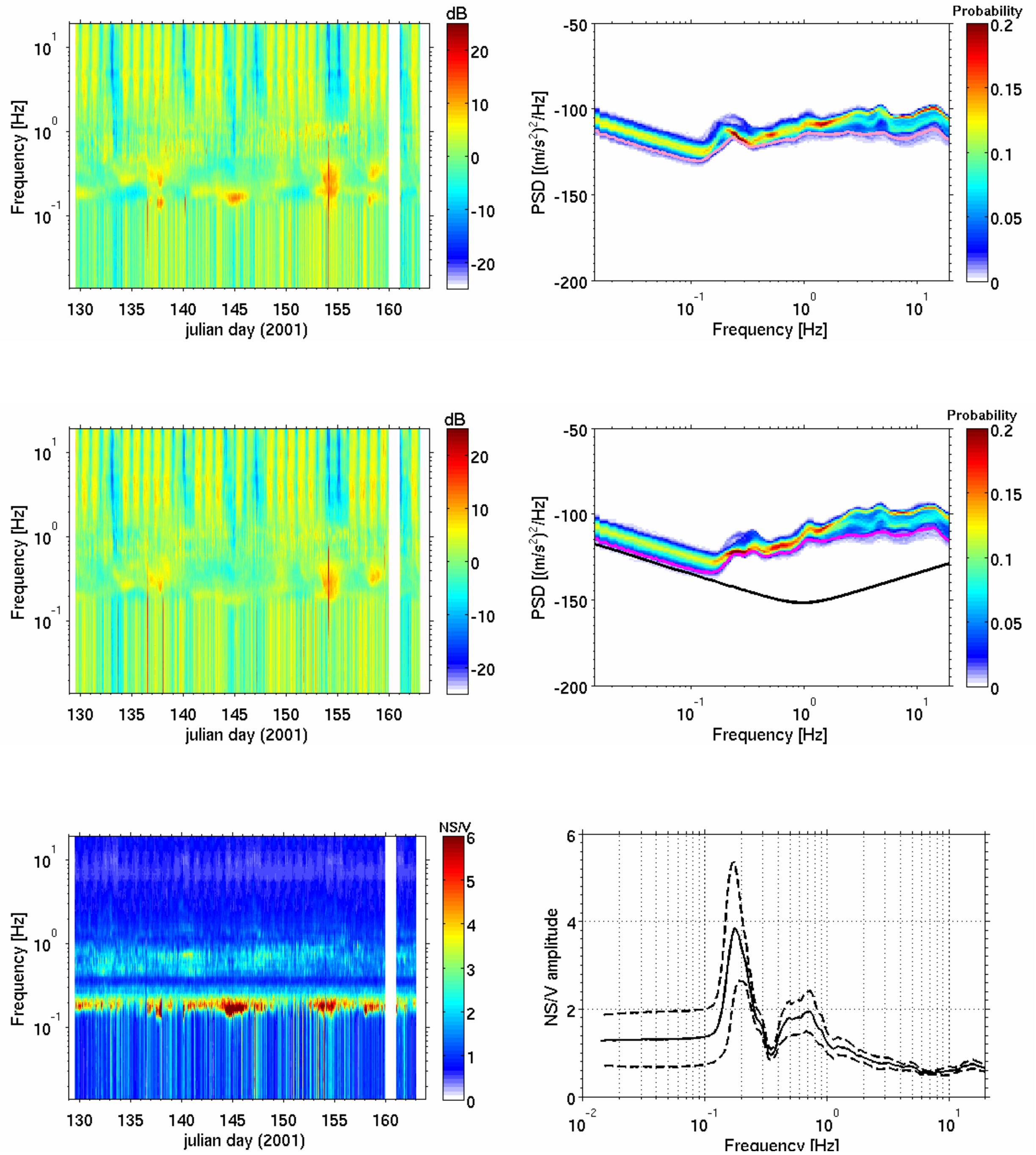
Frequency [Hz]
julian day (2001)
dB
PSD [(m/s^2)^2/Hz]
Frequency [Hz]
Probability
NS/V
NS/V amplitude

Figure 5

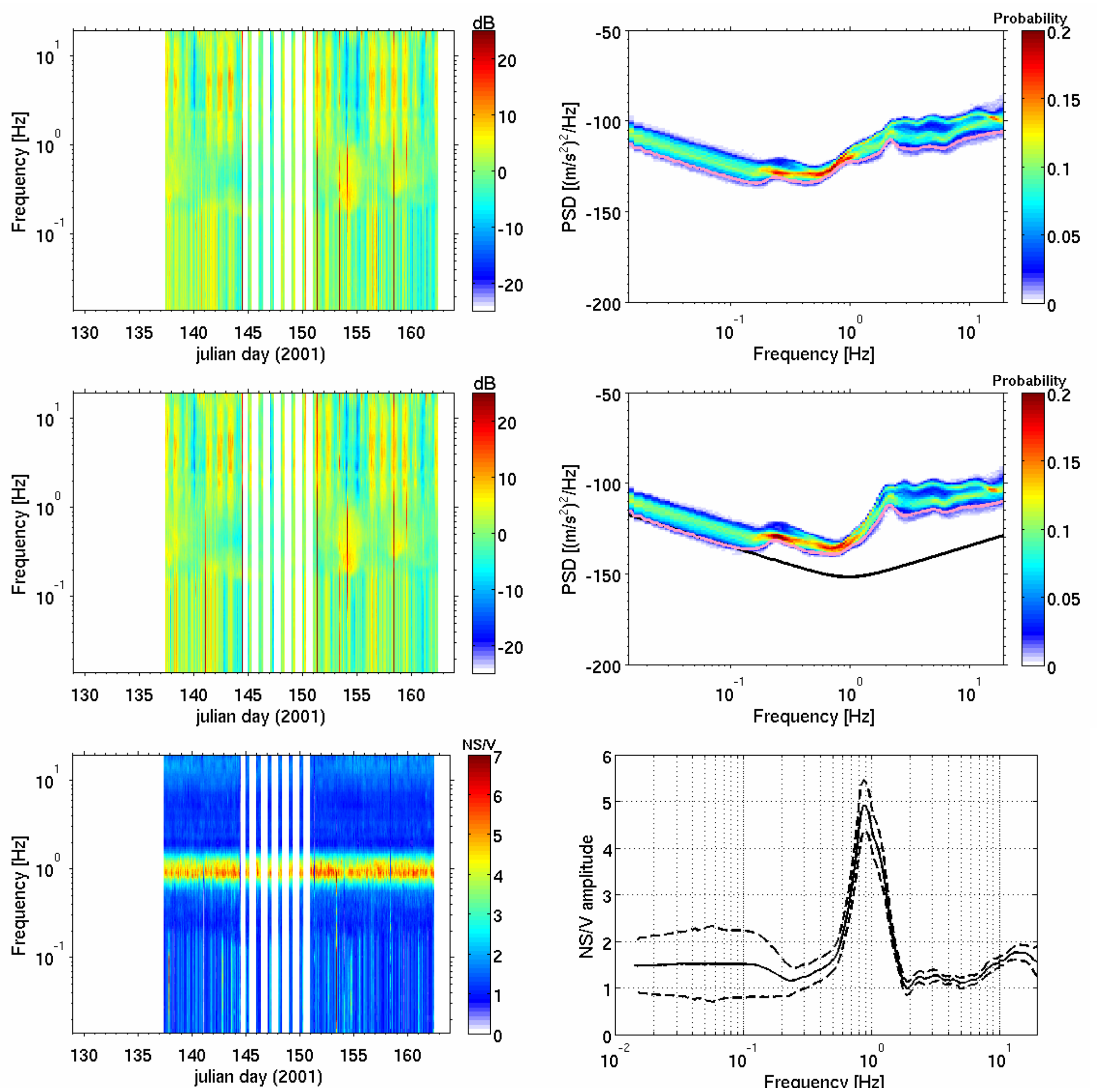
dB
Frequency [Hz]
julian day (2001)
Probability
PSD [(m/s²)²/Hz]
Frequency [Hz]
NS/V
NS/V amplitude

Figure 6

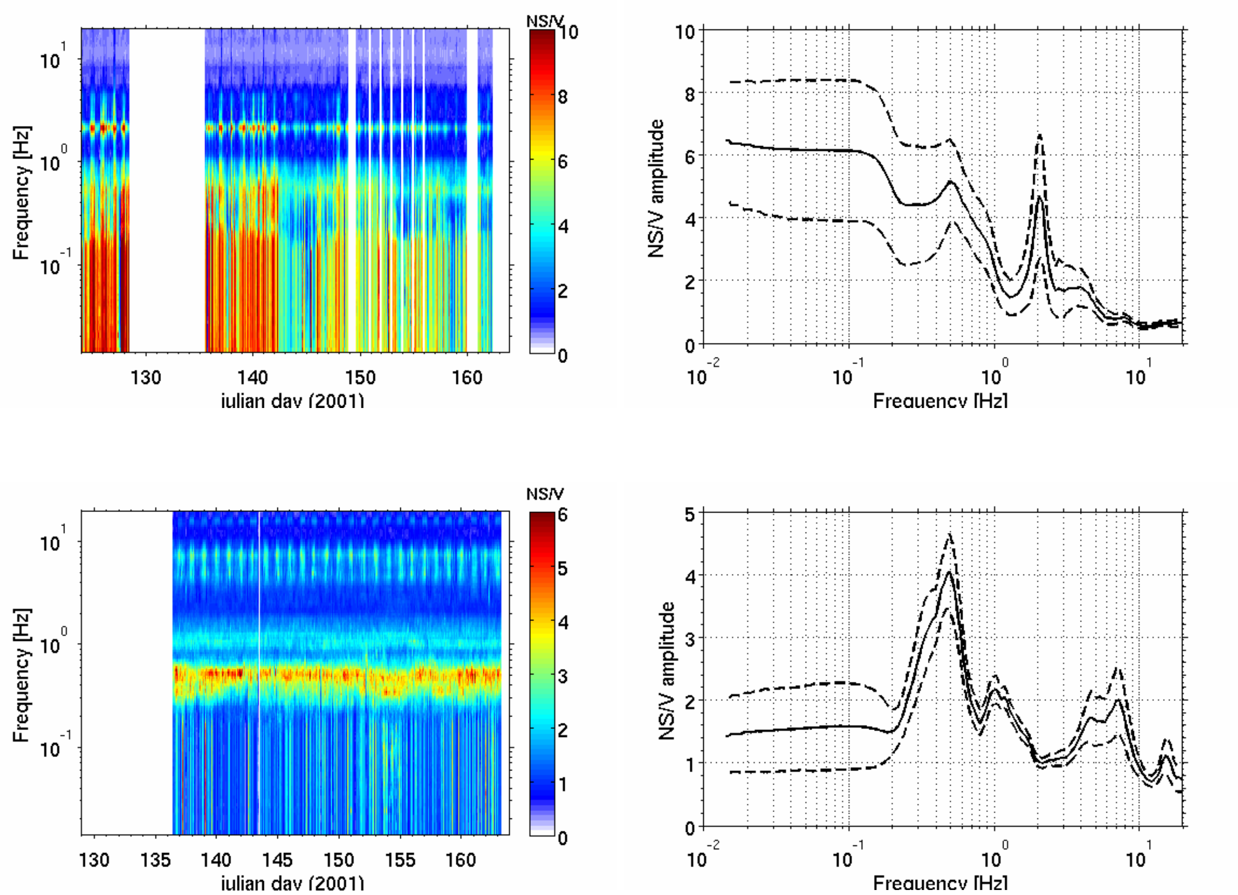
NS/V
Frequency [Hz]
julian day (2001)
NS/V amplitude
Frequency [Hz]

Figure 7

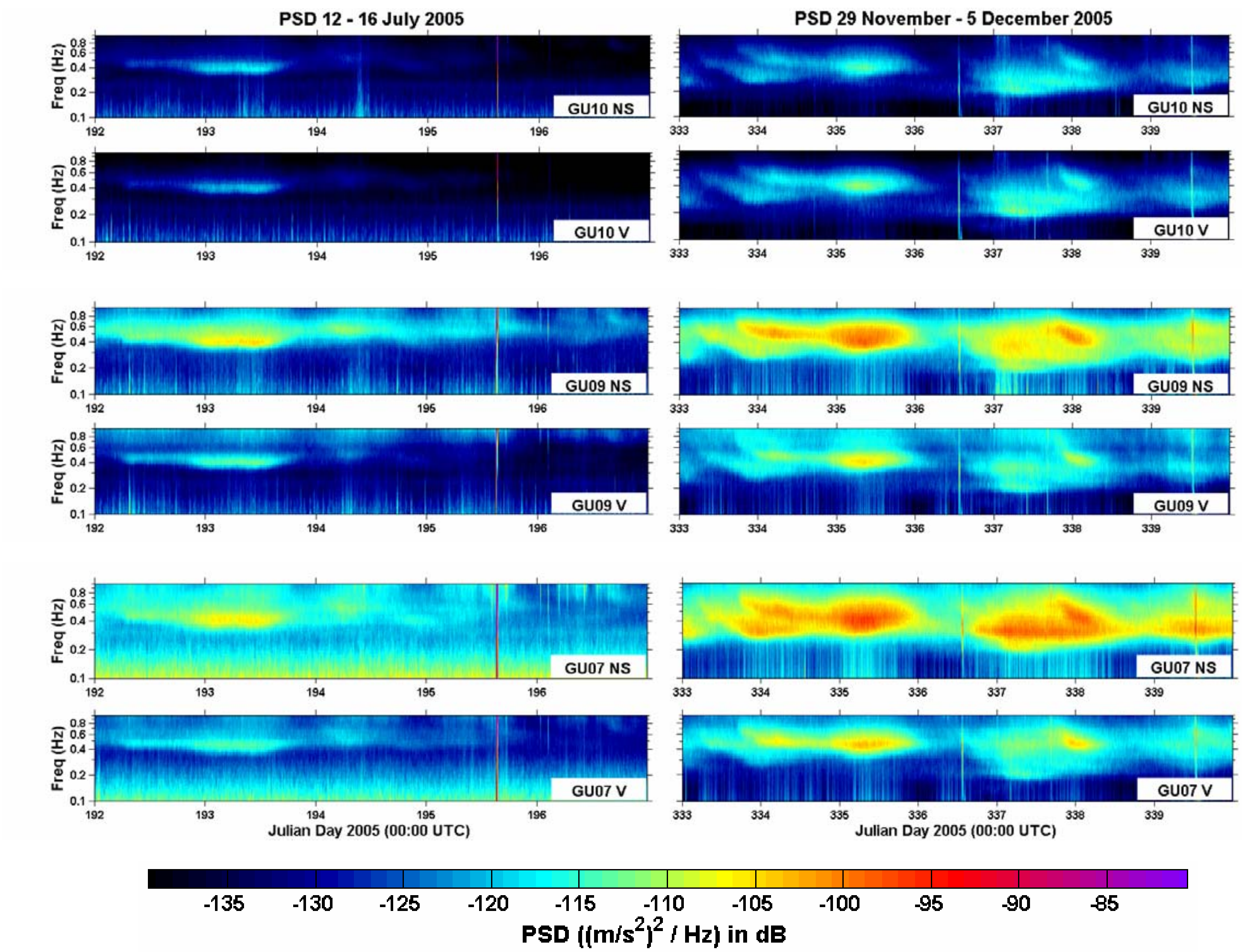
PSD 12 - 16 July 2005
PSD 29 November - 5 December 2005
Freq (Hz)
GU10 NS
GU10 V
GU09 NS
GU09 V
GU07 NS
GU07 V
Julian Day 2005 (00:00 UTC)
PSD ((m/s²)² / Hz) in dB

Figure 8

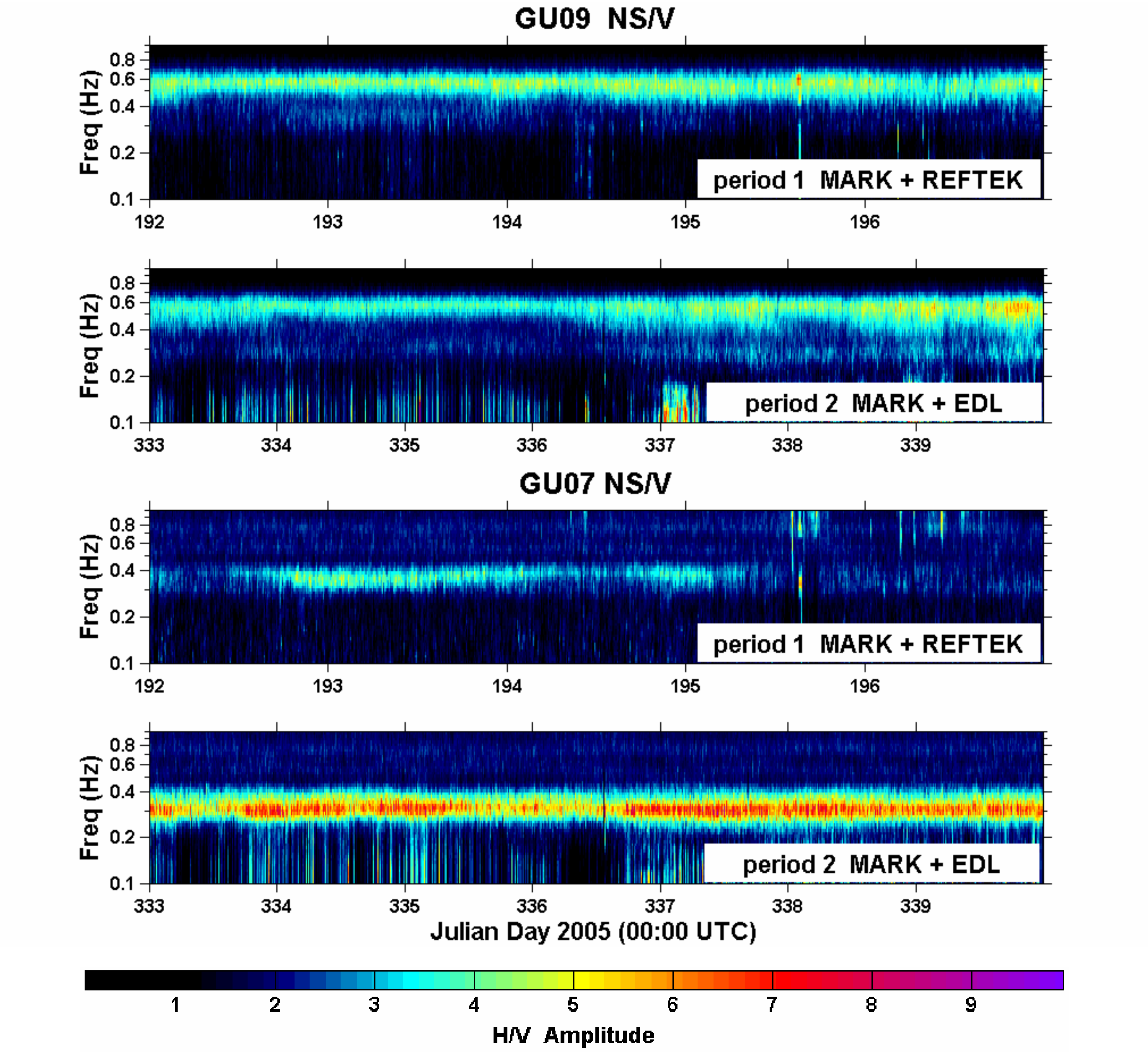
GU09 NS/V
Freq (Hz)
0.8
0.6
0.4
0.2
0.1
period 1 MARK + REFTEK
192
193
194
195
196
period 2 MARK + EDL
333
334
335
336
337
338
339
GU07 NS/V
Julian Day 2005 (00:00 UTC)
1
2
3
4
5
6
7
8
9
H/V Amplitude

Figure 9

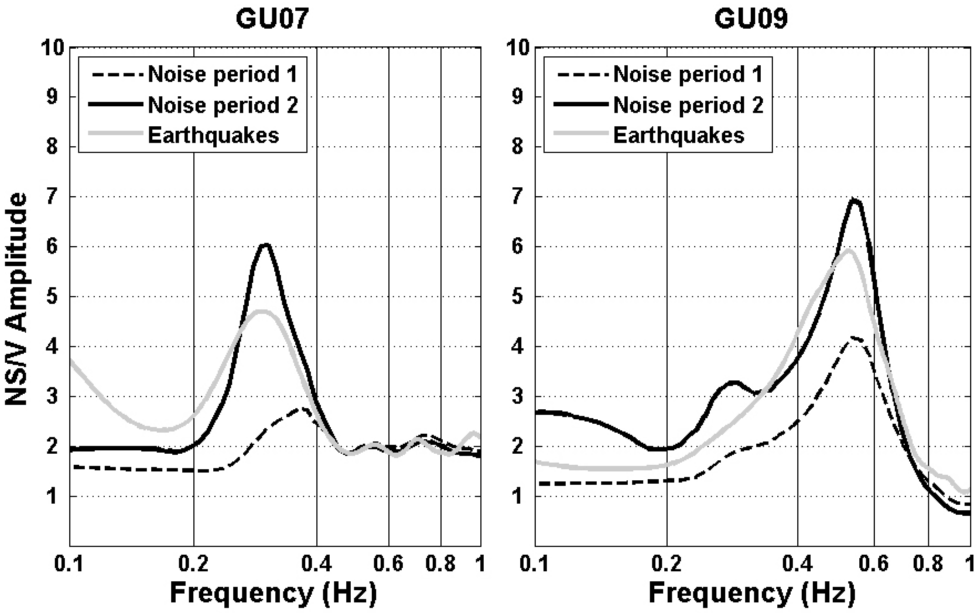

GU07
GU09
Noise period 1
Noise period 2
Earthquakes
NS/V Amplitude
Frequency (Hz)

Figure 10

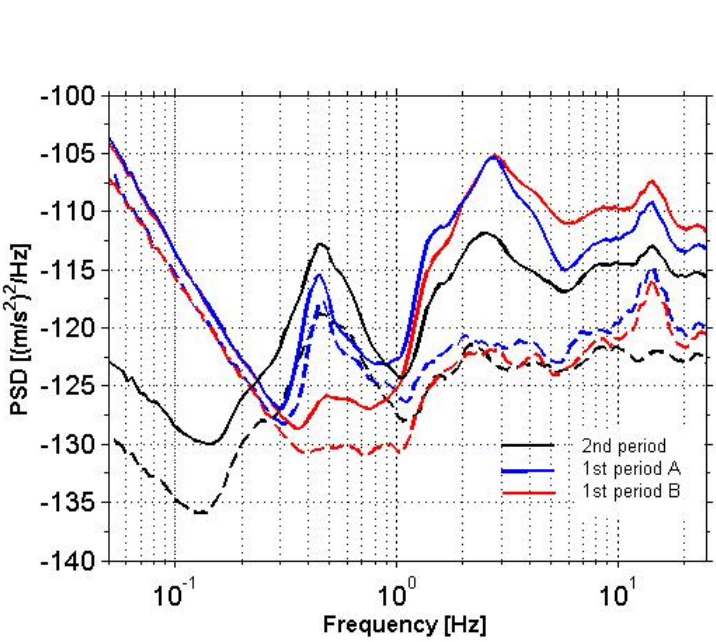
-100
-105
-110
-115
-120
-125
-130
-135
-140
PSD [(m/s^2)^2/Hz]
10^{-1}
10^{0}
10^{1}
Frequency [Hz]
2nd period
1st period A
1st period B

Figure 11